

First Results from the Third Level of the H1 Fast Track Trigger

A. W. Jung, A. Baird, R. Baldinger, S. Baumgartner, D. Beneckenstein, N. Berger, M.-O. Boenig, L. Caminada, D. Dodt, E. Elsen, M. Kolander, S. Kolya, K. Krüger, K. Lohwasser, D. Meer, D. Mercer, V. Michels, D. Müller, J. Müller, J. Naumann, P. R. Newman, D. Sankey, M. Sauter, A. Schöning, H.-C. Schultz-Coulon, M. Wessels, Ch. Wissing, W. Yan

Abstract—To make the best possible use of the higher luminosity provided by the upgraded HERA collider, the H1 collaboration has built the Fast Track Trigger (FTT). It is integrated in the first three levels (L1–L3) of the H1 trigger scheme and provides enhanced selectivity for events with charged particles.

The FTT allows the reconstruction of tracks in the central drift chambers down to 100 MeV. Within the 2.3 μs latency of the first trigger level coarse two dimensional track information in the plane transverse to the beam is provided. At the second trigger level (20 μs latency), high resolution, three dimensional tracks are reconstructed. Trigger decisions are derived from track momenta, multiplicities and topologies. At the third trigger level a farm of commercial PowerPC boards allows a partial event reconstruction. Within the L3 latency of 100 μs exclusive final states (e.g. D^* , J/ψ) are identified using track based invariant mass calculations. In addition an on-line particle identification of electrons and muons with additional information from other subdetectors is performed. First results obtained from the third level, which is fully operational since 2006, are presented.

Index Terms—Fast Track Trigger, on-line reconstruction, H1, HERA, real time, PPC, invariant mass, Track Trigger.

I. INTRODUCTION

The HERA accelerator at DESY collides 920 GeV protons with 27.6 GeV electrons (positrons) at a frequency of

A.W. Jung, KIP, Universität Heidelberg, Heidelberg, Germany
A. Baird, STFC Rutherford Appleton Lab., Oxfordshire, UK
R. Baldinger, ETH Zürich, Zürich, Switzerland
S. Baumgartner, ETH Zürich, Zürich, Switzerland
D. Beneckenstein, KIP, Universität Heidelberg, Heidelberg, Germany
N. Berger, ETH Zürich, Zürich, Switzerland
M.O. Boenig, Universität Dortmund, Dortmund, Germany
L. Caminada, ETH Zürich, Zürich, Switzerland
D. Dodt, Max-Planck-Institut für Plasmaphysik (IPP), Greifswald, Germany
E. Elsen, DESY, Hamburg, Germany
M. Kolander, Universität Dortmund, Dortmund, Germany
S. Kolya, University of Manchester, Manchester, UK
K. Krüger, KIP, Universität Heidelberg, Heidelberg, Germany
K. Lohwasser, University of Oxford, Oxford, UK
D. Meer, Paul Scherrer Institute, Villigen, Switzerland
D. Mercer, University of Manchester, Manchester, UK
V. Michels, DESY, Hamburg, Germany
D. Müller, SCS company, Zürich, Switzerland
J. Müller, SCS company, Zürich, Switzerland
J. Naumann, Universität Dortmund, Dortmund, Germany (left)
P.R. Newman, University of Birmingham, Birmingham, UK
D. Sankey, STFC Rutherford Appleton Lab., Oxfordshire, UK
M. Sauter, ETH Zürich, Zürich, Switzerland
A. Schöning, ETH Zürich, Zürich, Switzerland
H.C. Schultz-Coulon, KIP, Universität Heidelberg, Heidelberg, Germany
M. Wessels, DESY, Hamburg, Germany
Ch. Wissing, DESY, Hamburg, Germany
W. Yan, University of Cambridge, Cambridge, UK

10.4 MHz. To exploit the higher luminosity provided after the HERA machine upgrade the H1 experiment [1] has built a three level Fast Track Trigger FTT [2]. The task of the FTT system is to provide a high reduction factor to cope with the increased event rates at the upgraded HERA machine. The capability of the third trigger level (L3) to perform a track based on-line event reconstruction including invariant mass calculations and combinations of subsystem information offers the possibility to reduce the rates significantly. Constraints due to a fixed available rate budget for these exclusive triggers require large reduction factors whilst keeping a high efficiency for physics signals of interest. Some final state topologies that are selected by L3 and their corresponding event rates including previous trigger levels are given in table I.

decay channel	max. trigger rates [Hz]			L3 rate reduction
	L1	L2	L3	
$D^* \rightarrow K\pi\pi$ ($p_{t,D^*} > 1.5$ GeV)	500	90	5–7	≈ 13
$b \rightarrow eX$	500	90	2–3	≈ 30
inelastic $J/\psi \rightarrow e^+e^-$ ($\mu^+\mu^-$)	400	90	5–7	≈ 13

TABLE I

Trigger rates at L1, L2 and L3 are shown for some final state channels that are selected with FTT L3.

II. THE FTT LEVEL ONE AND TWO SYSTEMS

The FTT utilizes 12 wire layers out of the 56 wire layers of the H1 Central Jet Chambers as shown in figure 1. These 12

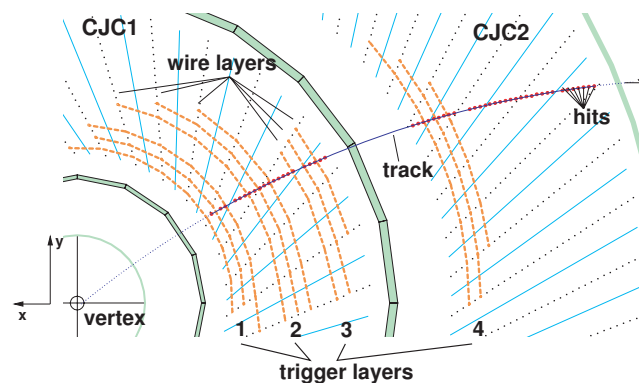


Fig. 1. The xy -plane of the H1 Central Jet Chambers (CJC1 & 2) is shown. The Fast Track Trigger (FTT) utilizes four groups of three wire layers out of the 56 wire layers of CJC1 & 2.

wire layers are organized in four trigger layers of three wire layers within which a search for track segments is performed. The analogue signals from both ends of the selected wires are digitized with a sampling rate of 80 MHz. Hits are identified by a fast Qt algorithm implemented in a FPGA. The z -position (along the beam and chamber wire direction) is determined using charge division [3].

At L1 track segments are found by filling the identified hits into shift registers. To reduce the bandwidth at level one an effective sampling rate of 20 MHz is used. The hit patterns are compared with pre-calculated, calibrated masks. The comparison is done in parallel using Content Addressable Memories (CAMs) performing $5 \cdot 10^{12}$ mask comparisons per second. If a track segment is found, the corresponding track curvature $\kappa = 1/p_t$ and the azimuthal angle ϕ are obtained from a look-up table. In a next step track segments are linked to L1 tracks. To this aim track segments from the four trigger layers are filled into four corresponding $\kappa\phi$ -histograms of the size 16×60 . A sliding window technique is used to link track segments to tracks by requiring a coincidence of at least 2 out of 4 trigger layers. Within the L1 latency of $2.3 \mu\text{s}$ trigger decisions based on the track multiplicity, the number of tracks above transverse momentum thresholds and the event topology are formed. A more detailed description of the FTT L1 system is given in [4] and [5].

In the L2 system [6], the full 80 MHz information is restored and used for validating the track segments found at L1. The linking step is repeated using histograms with 60×640 bins in the $\kappa\phi$ plane. As a coincidence of at least 2 out of 4 trigger layers precise two dimensional tracks are found. Afterwards the 3-dimensional hit information of the validated track segments is used by six Multi Purpose Boards (MPB [7], [8]) for a track fit [9]. For this purpose each MPB is equipped with four Floating-Point DSPs (TexasInstruments TMS320C6701).

A non-iterative helix track fit [10] uses the x - and y -positions of the track segments to determine κ and ϕ whereas a linear fit of the z -position of the track segments yields the polar angle θ . To improve the track parameter resolution a primary vertex constraint is applied. Each DSP performs up to two track fits. In total, FTT L2 can reconstruct up to 48 tracks per event which is sufficient for more than 98% of the events of interest. The resolution of the three track parameters ($1/p_t, \phi, \theta$) in comparison to off-line reconstructed central tracks is shown in figure 2. The peak resolutions determined by a fit are as follows: $\sigma_{\text{FTT}, 1/p_t} \approx 2.2\%/GeV$, $\sigma_{\text{FTT}, \phi} \approx 2.4 \text{ mrad}$ and $\sigma_{\text{FTT}, \theta} \approx 50 \text{ mrad}$. The fitted track parameters are sent to the 'L2 Decider' card where trigger decisions based on track multiplicities, event topology, transverse momenta and simple invariant mass calculations for less than eight tracks are formed. The L2 trigger decisions are sent to the central trigger within the L2 latency of $20 \mu\text{s}$.

The 'L2 Decider' forwards all track data together with other available trigger information in a fixed data transmission scheme via an LVDS [11] channel link (5 Gbit/s) running at 100 MHz to the L3 system. The transmitted data contain the L2 fitted track parameters, the reconstructed z -vertex position and L1 trigger information from other detector systems, like

the muon chambers and the calorimeter system.

III. THE FTT LEVEL THREE SYSTEM

Within the L3 latency of the H1 central trigger of about $100 \mu\text{s}$ a trigger decision based on invariant mass calculations and particle identifications is derived. The hardware of the third trigger level [12] consists of five (extendable up to 16) commercial VME PowerPCs [13] operated with the real time operating system vxWorks [14]. A schematic overview of the L3 system is shown in figure 3. The data are received on a LVDS channel link interface card ('SCS Piggy back card', [8]) attached to a custom made 'Receiver card'. The 'Receiver card' utilizing a single FPGA (Altera EP20K400) receives and buffers the L2 data. From the L3 'Receiver card' the data are distributed simultaneously to all PowerPC cards via a 20 MHz FPDP (Front Panel Data Port [15]) link (640 Mbit/s) using commercial 'PMC-DPIO cards' (PCI Mezzanine Cards [16]) attached to the PowerPCs. The PowerPCs are executing dedicated selection algorithms to derive trigger decisions. The communication with the central trigger is done with two dedicated input/output cards labelled as 'CTL interface card' and 'trigger bit card'. One 'master' VME PowerPC is used to control and read out the L3 system allowing off-line data consistency checks.

A. Data processing

A detailed sketch of the data processing and signal handling is shown in figure 4. The data are transmitted from the 'Receiver card' to the 'PMC-DPIO card' and via the PCI bridge to the PowerPC. The data processing is divided into three subsequent 'steps' which consist of several threads:

- 1) the data transmission step,
- 2) the preparation step,
- 3) the selection step.

The inter process communication and synchronization is done using special signals called semaphores provided by the real time operating system. A semaphore has - to first approximation - two different states, 'locked' or 'unlocked', and is able to control threads with different priorities as used in the three processing steps. In addition they guarantee a fast and prompt answer to interrupts necessary to ensure decisions within the $100 \mu\text{s}$ L3 latency.

The data transmission step contains the reception of the L2 data and the data distribution within the L3 system. The reception of the first word of the L2 event data by the FIFO on the 'PMC-DPIO card' is indicated to the CPU of the PowerPC via a PCI interrupt. This interrupt initiates a Direct Memory Access (DMA) transfer of the content of the FIFO to a dedicated memory address. The end of the DMA data transfer is marked by an end of transfer interrupt (EOT-IR) delivered by the 'PMC-DPIO card'. With the EOT-IR the data preparation step starts.

First an on-line consistency check of the transmitted data is performed. Afterwards the data preparation step converts them into the format used by the selection algorithms. As soon as the data preparation has finished the third processing step is released running the different selection algorithms.

The first two processing steps are identical on every PowerPC whereas the third processing step is specific and contains physics selection algorithms which are discussed in section IV. Modifications to the executed selection algorithms are documented by version numbers stored to the H1 database. This allows the off-line verification of the FTT trigger decision as well as trigger simulations taking the actual trigger settings and selection algorithms into account.

B. Optimizations and latency constraints

The simultaneous data transfer to the 'PMC-DPIO cards' from the 'Receiver card' ensures data transmissions within 10 μs . The time used to transfer the data from the FIFO of the 'PMC-DPIO card' to the memory of the PowerPCs using the fast DMA access is negligible. Key factors for the L3 software design are a minimal interrupt latency and a short thread switching latency. A real time operating system like vxWorks fulfills these requirements.

In the preparation step, kinematic and other variables are calculated that are used by the various selection algorithms. This includes the calculation of the momentum components p_x, p_y, p_z from $1/p_t, \phi, \cot(\theta)$ delivered by the L2 track fit. Energies of tracks are calculated for all those particle mass hypotheses which are later used in the invariant mass calculation. To reduce the preparation time Taylor approximations for trigonometrical functions are used. In addition the track look-up for the muon identification is made. The preparation step needs up to 30 μs leaving about 60 μs for the actual selection algorithms running in the selection step where e.g. invariant masses are calculated. In order to be fast, the equations used by the selection algorithms contain e.g. squared terms instead of square roots and Taylor approximations wherever possible. The time consumption for each step is shown in figure 5 as function of the number of tracks for the D^* selection algorithm (see section IV). The dotted line shows the data transmission time to the L3 PowerPC boards with up to 10 μs . The data preparation time is shown as dash-dotted line with up to 30 μs . The total time consumption for this selection algorithm is shown in figure 5 as colored area. For 97% of the events of interest the algorithm terminates within the given latency of 100 μs .

IV. PHYSICS ALGORITHMS

Within the L3 system various selection algorithms are used to identify exclusive final states on-line. The following selection algorithms are implemented:

- D^* mesons with different p_t -thresholds
- inelastic J/ψ mesons with different p_t -thresholds
- diffractive vector mesons
- electron identification with different p_t -thresholds
- muon identification.

The first three selections are purely track based whereas the last two selections are using L1 trigger information from the calorimeter and muon systems. The main focus of the FTT L3 system is on the identification of rare processes containing c - and b -quarks in a regime with high backgrounds from other ep scattering processes, demanding high selectivity and precision.

Two example applications are discussed. First the on-line D^* selection including a discussion of first results, second the on-line particle identification for electrons and muons is presented.

A. Identification of D^* mesons at L3

The selection of D^* mesons is done in the so called 'golden decay' channel ($D^* \rightarrow D^0 \pi_{\text{slow}} \rightarrow K \pi \pi_{\text{slow}}$) which can be fully reconstructed from charged particles. For the on-line identification of D^* mesons no particle identification is applied, thus increasing combinatorics. However, the combinatorial background can be reduced by first reconstructing the D^0 candidate and then the D^* candidate.

The D^0 is reconstructed by assuming one track to be a kaon and the other to be a pion with opposite charge. If the two candidates have a transverse momentum above a certain threshold an invariant mass hypothesis is calculated. Those $K\pi$ pairs having an invariant mass consistent with the D^0 mass hypothesis are sequentially combined with a third track (' π_{slow} ') which has to have a charge of opposite sign to that of the kaon candidate and to which the pion mass hypothesis is assigned. The small value of the mass difference $\Delta M = M(K\pi\pi_{\text{slow}}) - M(K\pi)$ implies a very low momentum for the π_{slow} . As shown in figure 6 a D^* candidate is found as a distinct narrow enhancement in the distribution of the mass difference $\Delta M = M(K\pi\pi_{\text{slow}}) - M(K\pi)$ around the expected value of 145.4 MeV [17]. The ΔM method is highly effective in the removal of background processes. For the D^* identification an upper ΔM cut is applied and a transverse momentum of the D^* (p_{t,D^*}) above a certain threshold is required. If a candidate passes the cut a positive trigger decision is sent to the central trigger. Otherwise the next possible track combination is tried until all possible track combinations have been tested. To visualize the D^* selection capabilities of the FTT the on-line ΔM distribution is compared to the one reconstructed off-line as shown in figure 6. The on-line ΔM distribution is only shown for those D^* candidates within the signal region of the off-line ΔM distribution. The on-line ΔM distribution demonstrates that the resolution of the L2 fitted tracks is sufficient for the on-line identification of D^* mesons at FTT L3. Two different ΔM cuts with $\Delta M < 0.180$ GeV and $\Delta M < 0.280$ GeV are used. In order to cope with varying beam and background conditions and in order to fully exploit the delivered luminosity under given bandwidth limitations three exclusive D^* triggers with p_{t,D^*} -thresholds of 1.5, 2.5 and 4.5 GeV have been set up. The efficiency of the L3 D^* identification as function of p_{t,D^*} obtained from an independently triggered D^* sample is shown in figure 7 for the three different p_{t,D^*} -thresholds. The efficiency for all three D^* triggers starting at a transverse momentum as low as 1.5 GeV up to 14 GeV is about 45% – 50%.

The achieved rate reduction factors and the corresponding efficiencies are summarized in table II. For instance a p_{t,D^*} -threshold of 4.5 GeV gives a rate reduction factor of about 60 whereas the lowest p_{t,D^*} -threshold of 1.5 GeV gives a rate reduction factor of about 13.

p_{t,D^*} -threshold	efficiency	max. L3 rates [Hz]	L3 rate reduction
> 1.5 GeV	0.50	5 – 7	≈ 13
> 2.5 GeV	0.45	1.0 – 1.5	≈ 40
> 4.5 GeV	0.45	0.8 – 1.0	≈ 60

TABLE II

Efficiencies for different p_{t,D^*} -thresholds and their corresponding trigger rates and rate reduction factors as achieved with FTT L3.

The D^* sample as selected by FTT L3 and reconstructed off-line is shown in figure 8 where all three D^* triggers were combined. The fit yields (11939 ± 232) D^* mesons which is an order of magnitude more compared to previous H1 datasets [18].

B. Identification of electrons in L3

The L3 electron identification is designed to trigger electrons with energies as low as 1.2 GeV, much lower than the threshold for the inclusive H1 electron triggers of about 5 GeV. This gives access to electrons stemming from decays of low momentum b-quarks. The idea of the L3 electron trigger is to match the FTT track geometrically and kinematically to the energy measurement of the calorimeter trigger (jet trigger). The jet trigger is sensitive to low energy depositions and provides good topological information. A geometrical match is done by allocating to every FTT track a jet trigger cluster in an acceptance window as illustrated in figure 9. The main focus is on discriminating electrons from high energetic pions. In a non-compensating calorimeter (like the H1 Liquid-Argon Calorimeter), the detectable energy is smaller for hadrons than for electrons. Therefore, a lower cut on the E_t/p_t ratio (transverse energy measured by the jet trigger divided by the FTT measured transverse momentum of the tracks) permits a coarse distinction of electrons and charged hadrons. Background originating from π^0 decays in jets is largely reduced by requiring a good geometrical match between the FTT track and the energy deposition in the calorimeter.

The performance of the L3 electron trigger in data is checked with the decay $J/\psi \rightarrow e^+e^-$. The signature of these events is suitable as it contains only two isolated electrons with a transverse momentum of typically 1 – 3 GeV which covers the range of the implemented L3 electron triggers. Figure 10 shows the L3 electron identification efficiency for two single tag electron finder with a medium (1.5 GeV) and a high (2.0 GeV) p_t -threshold and for a double tag electron finder with a low (1.2 GeV) p_t -threshold. The rate reduction achieved ranges from a factor of 15 for the medium p_t -threshold to 100 for the high p_t -threshold. Only with a double tag electron finder it is possible to go to the lowest p_t -threshold of 1.2 GeV. Because of using somewhat relaxed cuts a higher electron identification efficiency is achieved for the double tag electron finder compared to the single tag electron finders, see figure 10.

C. Identification of muons in L3

The L3 muon identification is performed by validating FTT tracks with L1 information received from the muon trigger

system. The main focus is to increase the discrimination between muons originating from the ep interaction vertex and cosmic muons.

The muon system consists of streamer tubes which are located inside and around the iron return yoke of the H1 magnet. The muon system is divided into 64 modules. Using a FTT track look-up table triggered muon modules are validated assuming that the FTT track is a muon originating from the ep -interaction point. The event is accepted if at least one L1 triggered muon module is validated by a FTT track. The principle is illustrated with a sketch of the muon system in the $\theta\phi$ -plane containing four tracks (including one muon in module 21) as shown in figure 11.

The efficiency of the L3 identification for isolated muons was verified using the decay $J/\psi \rightarrow \mu^+\mu^-$ to be above 98% ($p_t > 1.7$ GeV). The rate reduction achieved is between a factor of 3 for the barrel region and 10 for the endcap region. The muon identification of L3 provides a better background rejection for cosmic muons. In addition extra regions of the muon trigger system that suffered from beam background could be included and the global muon trigger rate could be considerably reduced, thus opening bandwidth for other triggers.

V. CONCLUSION

The FTT is a three level trigger system providing coarse track information at the first trigger level within $2.3 \mu s$ and precise track information at the second trigger level within $20 \mu s$. A full event analysis and a selection of track based exclusive final states is performed at the third trigger level within $100 \mu s$. By combining track information with other H1 trigger subsystems electrons and muons can be identified on-line. All three levels of the FTT system are in full operation since 2006 and fulfill the specification.

First results were obtained by the FTT L3 system and presented here. High performances are achieved for triggering D^* mesons using the golden decay channel and for triggering electrons and muons from b-quark decays using particle identification algorithms. Large data samples collected by those triggers will permit complementary measurements of the gluon density of the proton in charm and beauty production in an extended kinematic region at lowest transverse momenta.

REFERENCES

- [1] I. Abt et al., *The H1 Detector at HERA*, Nucl. Instr. and Meth., vol. A386, pp.310 & 348, 1997.
- [2] A. Baird et al., *A fast high resolution track trigger for the H1 experiment*, IEEE Trans. Nucl. Sci., vol. 48, pp. 1276-1285, 2001.
- [3] A. Schöning, *A fast track trigger for the H1 collaboration*, Nucl. Instrum. Meth., vol. A518, pp. 542-543, 2004.
- [4] N. Berger et al., *First Results from the First Level of the H1 Fast Track Trigger*, Proc. of the 2004 NSS Symposium, Oct. 2004, Rome, Italy.
- [5] Y.H. Fleming, *The H1 First Level Fast Track Trigger*, Ph.D., 2003, Univ. of Birmingham, UK.
- [6] Ch. Wissing et al., *Performance of the H1 Fast Track Trigger Operation and Commissioning Results*, Proc. of the 14th IEEE - NPSS Real time Conference 2005, p233-236, Stockholm, Sweden.
- [7] D. Meer et al., *A multifunctional processing board for the fast track trigger of the H1 experiment*, IEEE Trans. Nucl. Sci., vol. 49, pp. 357-361, 2002.

- [8] SCS Supercomputing Systems, company, Zürich, Switzerland.
- [9] Ch. Wissing, *Entwicklung eines Simulationsprogrammes und Implementierung schneller Spuralgorithmen für den neuen H1-Driftkammertrigger*, Dissertation, Universität Dortmund, 2003, Germany.
- [10] V. Karimäki, *Effective circle fitting for particle trajectories*, Nucl. Instr. and Meth., vol. A305, pp. 187, 1991.
- [11] National Semiconductor, <http://www.national.com>, data sheet DS90CR483/484: 48 bit LVDS channel link Serializer/Deserializer, July 2000.
- [12] J. Naumann, *Entwicklung und Test der dritten H1-Triggerstufe*, Dissertation, Universität Dortmund, 2003, Germany.
- [13] Motorola, <http://www.freescale.com>, data sheet MVME2400: single CPU VME board, July 2000.
- [14] Wind River System Inc., *vxWorks Programmers Guide, 5.4*, Edition 1, 1999.
- [15] ANSI/VITA 17-1998 (Front Panel Data Port).
- [16] IEEE P1386.1 (PMC Mezzanine card).
- [17] W. Yao, et al., *Review of particle physics*, J. Phys., G33 pp. 1-1232, 2006.
- [18] A. Aktas et al., *Inclusive D*-Meson Cross Sections and D*-Jet Correlations in Photoproduction at HERA*, Eur. Phys. J.C , vol. 50 No. 2, pp. 251-269, August 2006.

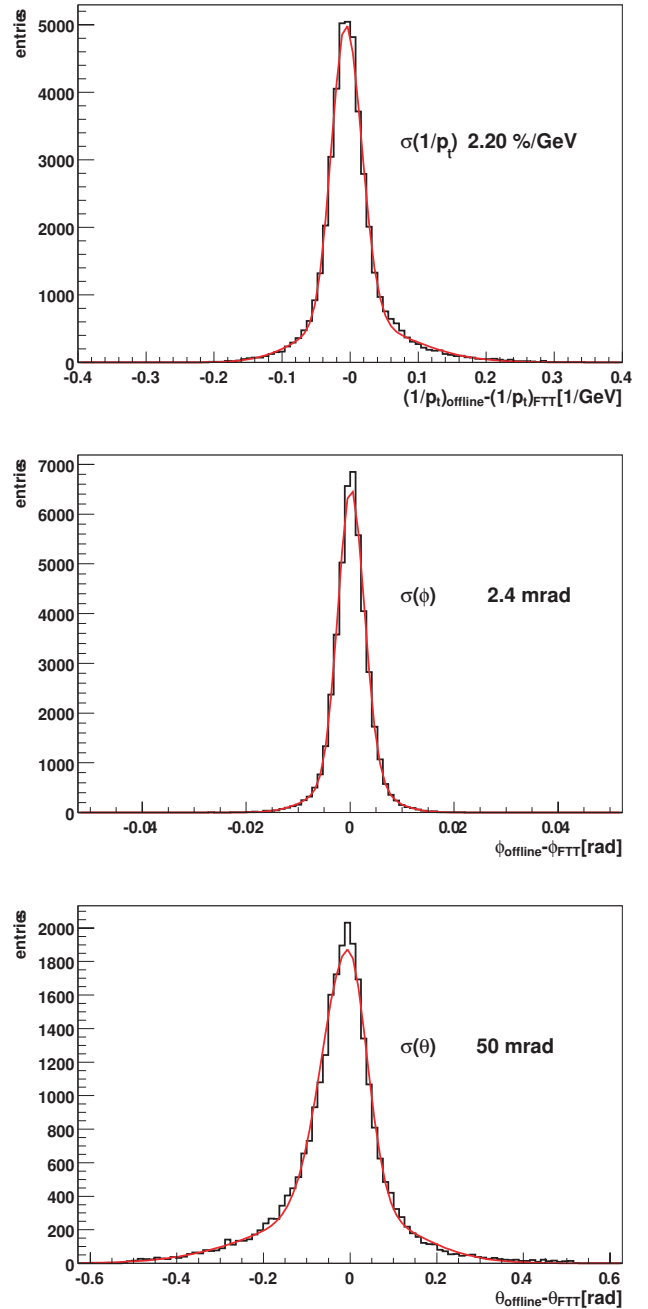


Fig. 2. The resolution σ of the FTT L2 track parameters $1/p_t = \kappa$, ϕ and θ compared to the off-line reconstructed tracks.

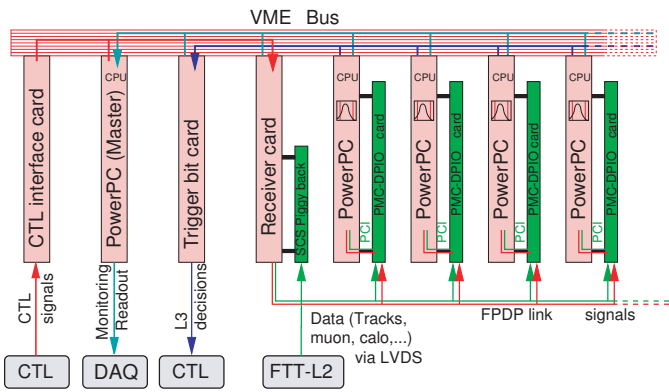


Fig. 3. Schematic view of the L3 system with the data and signal lines. For a detailed description see text.

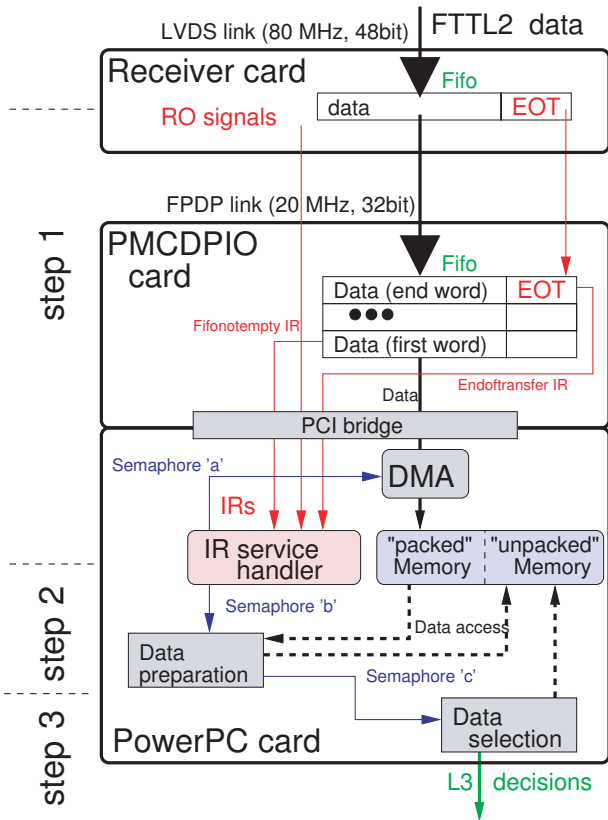


Fig. 4. Schematic view of the data transmission and processing within the L3 system from the 'Receiver card' to the 'PMC-DPIO card' and finally to the PowerPC. The semaphores are part of the inter process communication of the threads used in the software of the PowerPCs.

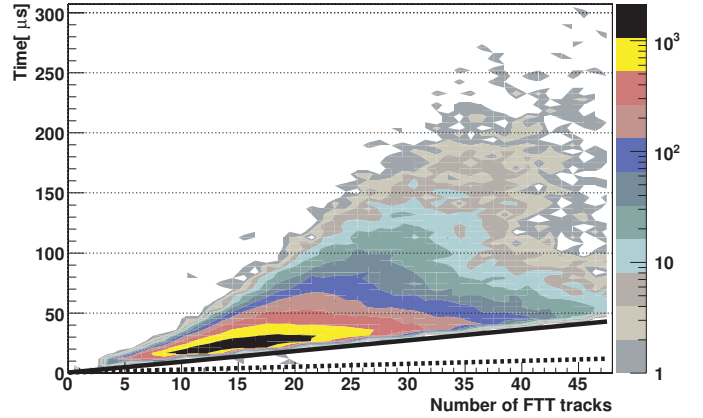


Fig. 5. The L3 time consumption is shown for the D^* selection algorithm. The dotted line shows the data transmission time to the L3 PowerPC boards. The data preparation time is shown as dash-dotted line whereas the overall time consumption including the selection algorithm is shown as the colored area.

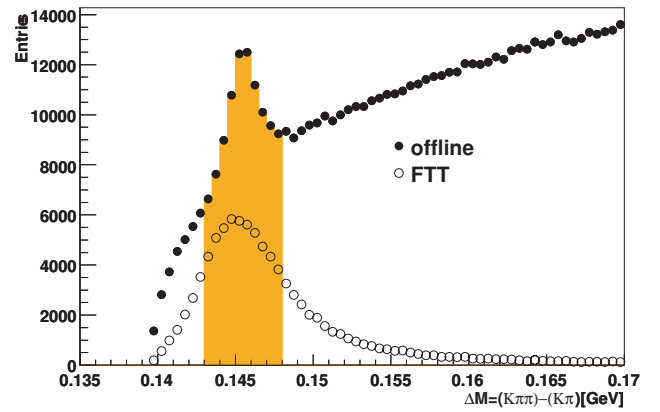


Fig. 6. The on-line FTT ΔM distribution (open circles) that is derived from the signal region (shaded area) of the off-line reconstructed sample (closed circles) is shown demonstrating the good resolution of the FTT.

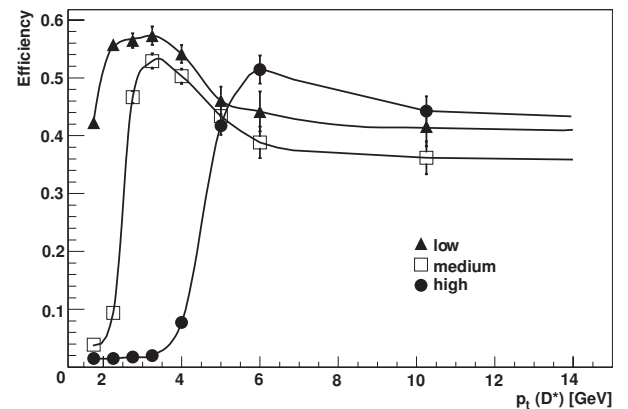


Fig. 7. The L3 efficiency for the on-line identification of a D^* as function of p_{t,D^*} is shown for the low (filled), medium (open) and high (circle) p_{t,D^*} trigger corresponding to thresholds of $p_{t,D^*} > 1.5, 2.5$ and 4.5 GeV (The black lines are just to guide the eyes.)

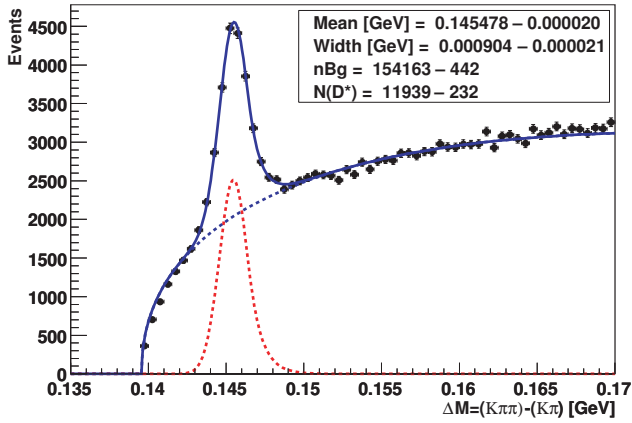


Fig. 8. The D^* meson peak in the off-line reconstructed ΔM distribution of FTT L3 triggered events. The parameters of the fit are given in the box. In total (11939 ± 232) D^* s are identified.

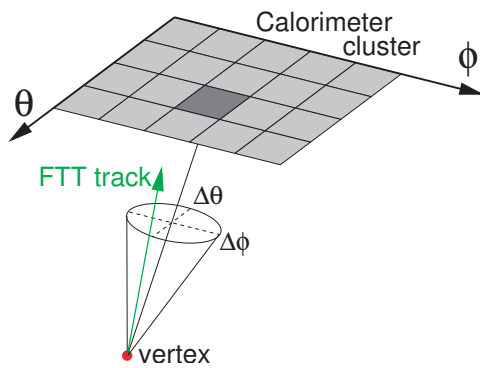


Fig. 9. The electron identification is done by allocating to every FTT track a (triggered) calorimeter cluster in an acceptance window determined by $\Delta\theta$ and $\Delta\phi$.

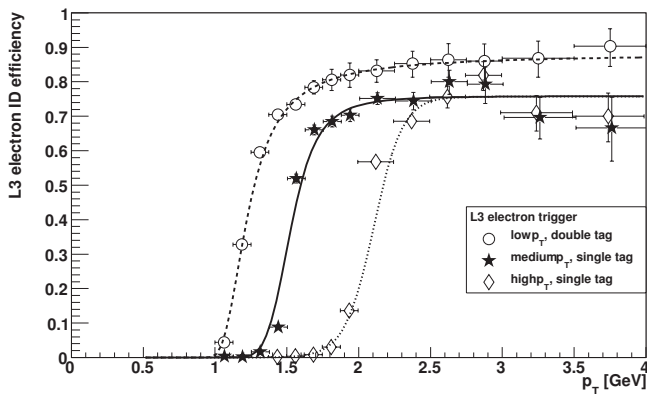


Fig. 10. The L3 electron identification efficiency of the single tag medium and high p_t electron finder (filled stars/open diamonds) as function of p_t . The double tag electron finder (open circles) with the lowest p_t -threshold for the electron is shown. The different p_t -thresholds of 1.2, 1.5 and 2.0 GeV are clearly visible. (For visibility reasons the horizontal bin centers are slightly shifted.)

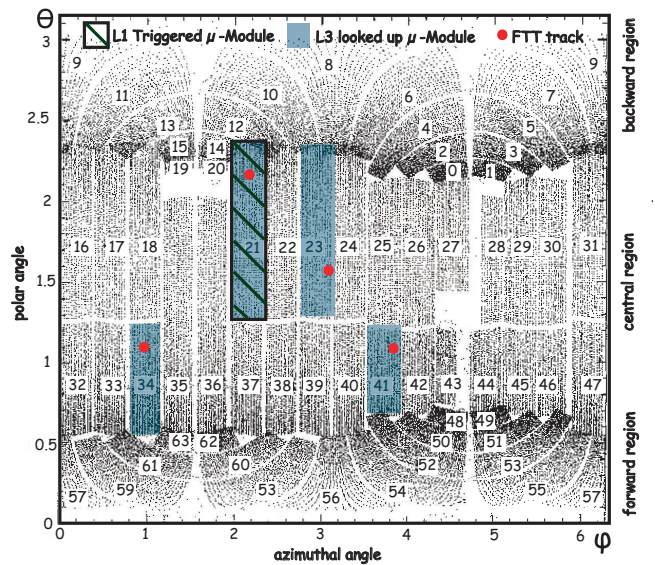


Fig. 11. Hit map of the central muon system. The numbers label the 64 different modules. The basic ideas of the L3 muon identification are illustrated: The thick points refer to FTT tracks extrapolated to the muon system. The corresponding muon modules are shaded. The L1 triggered module 21 is hatched in black. If one module with a positive L1 trigger decision is also identified by the look-up table applied to FTT tracks the event is accepted.